WAVELET-BASED MOTION ARTIFACT REMOVAL FOR ELECTRODERMAL ACTIVITY

Weixuan Chen*, Natasha Jaques*, Sara Taylor*, Akane Sano*, Szymon Fedor* and Rosalind W. Picard*
*Affective Computing Group, MIT Media Lab, 75 Amherst Street, Cambridge, U.S.
{cvx, jaquesn, sataylor, akanes, sfedor, picard}@media.mit.edu

Electrodermal Activity

- Electrodermal activity (EDA) refers to the changes of the electrical properties of the skin in response to sudomotor innervation [3], which can be recorded as skin conductance (SC) [7].
- Because SC provides a fine measure of the sympathetic nervous system (SNS) activity, it is widely used in psychophysiology as an indication of psychological or physiological arousal.

Figure 1. An ambulatory EDA sensor (Q sensor, Affectiva, Inc.).

Motion Artifact in EDA

- Analysis of EDA is hampered by its sensitivity to motion artifacts, even when subjects are asked to avoid gross body movements.
- As ambulatory EDA sensors are adopted in more and more studies related to affective phenomena [9, 10], sleep [17], epilepsy [16] and stress [8, 11], removing motion artifacts before further statistical treatment becomes even more essential.
- One of the most common artifacts in EDA is unusual steep rises (see Fig. 2), stemming from pressure exerted on the electrodes [5].

Previous Methods

- There are a few methods previously taken to correct motion artifacts, such as exponential smoothing [11] and other low-pass filters [12, 15, 16].
- However, these non-adaptive methods are unable to compensate for artifacts abruptly appearing with much larger intensity than EDA, and the whole time series are filtered indiscriminately, which may distort SC signals without artifacts.

Our Method

A. Stationary wavelet transform

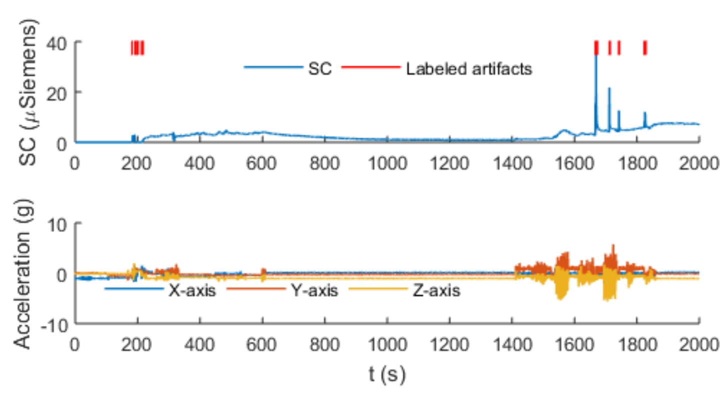

Figure 2. SC signal with motion artifacts labeled by two expert EDA researchers; Actigraph in three axes.

- SWT decomposition of a signal y(t) results in the scaling (approximation) and wavelet (detail) coefficients:

$$c_{2^j}^{2^jk+p} = < y(t), 2^{-j/2}\phi(\frac{t-p}{2^j}-k) >$$

$$d_{2^j}^{2^jk+p} = < y(t), 2^{-j/2}\psi(\frac{t-p}{2^j}-k) >$$

Here we chose j = 1, ..., 8, which means EDA data were decomposed into 8 levels.

- Distribution of wavelet coefficients can be modeled as a mixture of two Gaussians [1], [4]. This model fits the characteristics of SC signals well. Time series of SC can be characterized by a slowly varying tonic activity (i.e., skin conductance level; SCL) and a fast varying phasic activity(i.e., skin conductance responses; SCRs) [2]. In summary, the wavelet coefficients of an observed SC signal y(t) can be written as

$$d_{2^j}^{2^jk+p} = \bar{d}_{2^j}^{2^jk+p} + \varepsilon_{2^j}^{2^jk+p}$$

$$d_{2^j}^{2^jk+p} \sim \gamma_j N(0, \sigma_j^2) + (1-\gamma_j) N(0, c_j^2\sigma_j^2)$$

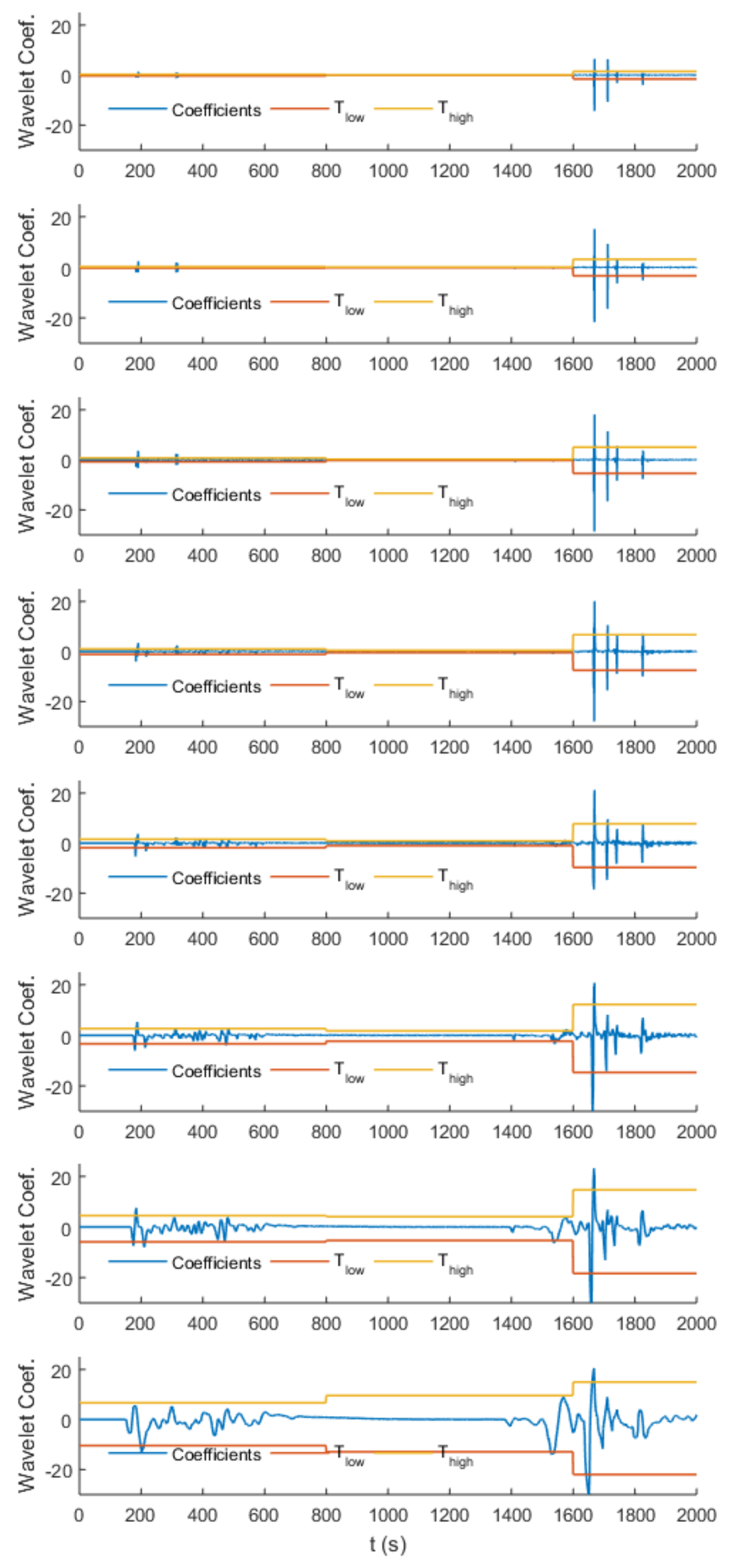

Figure 3. 8 levels of wavelet coefficients with adaptive thresholds.

C. Inverse wavelet transform

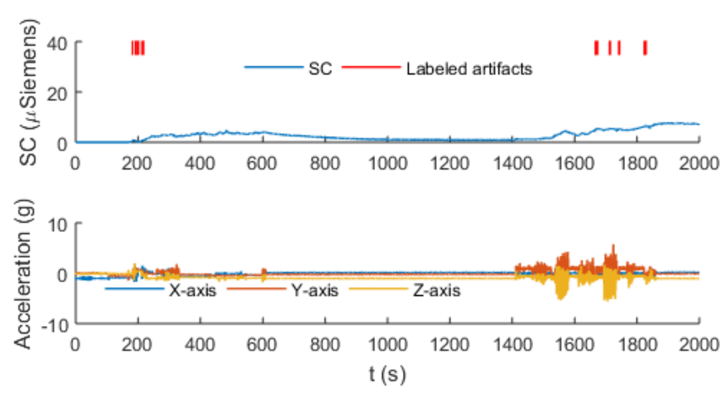

Figure 4. Denoised SC signal with motion artifacts labels; Actigraph in three axes.

Assuming ε takes up a very small proportion, from the wavelet coefficients of the original signal d, γ_j, σ_j and c_j can be estimated for each level j using an Expectation Maximization (EM) algorithm [13].

- Assume the proportion of ε in d is δ (the artifact proportion). For any given wavelet coefficient, if the probability of observing values smaller or larger than it is less than δ/2, we can conclude that the coefficient does not belong to the valid SC and should be a result of motion artifacts. Therefore,

$$\Phi(T_{low}) = 1 - \Phi(T_{high}) = \delta/2$$

- Finally, motion artifacts can be removed from the wavelet coefficients using the following scheme:

$$\hat{d}_{2^j}^{2^jk+p} = \begin{cases} d_{2^j}^{2^jk+p} & if\ T_{low} < d_{2^j}^{2^jk+p} < T_{high} \\ 0 & otherwise \end{cases}$$

B. Adaptive thresholding

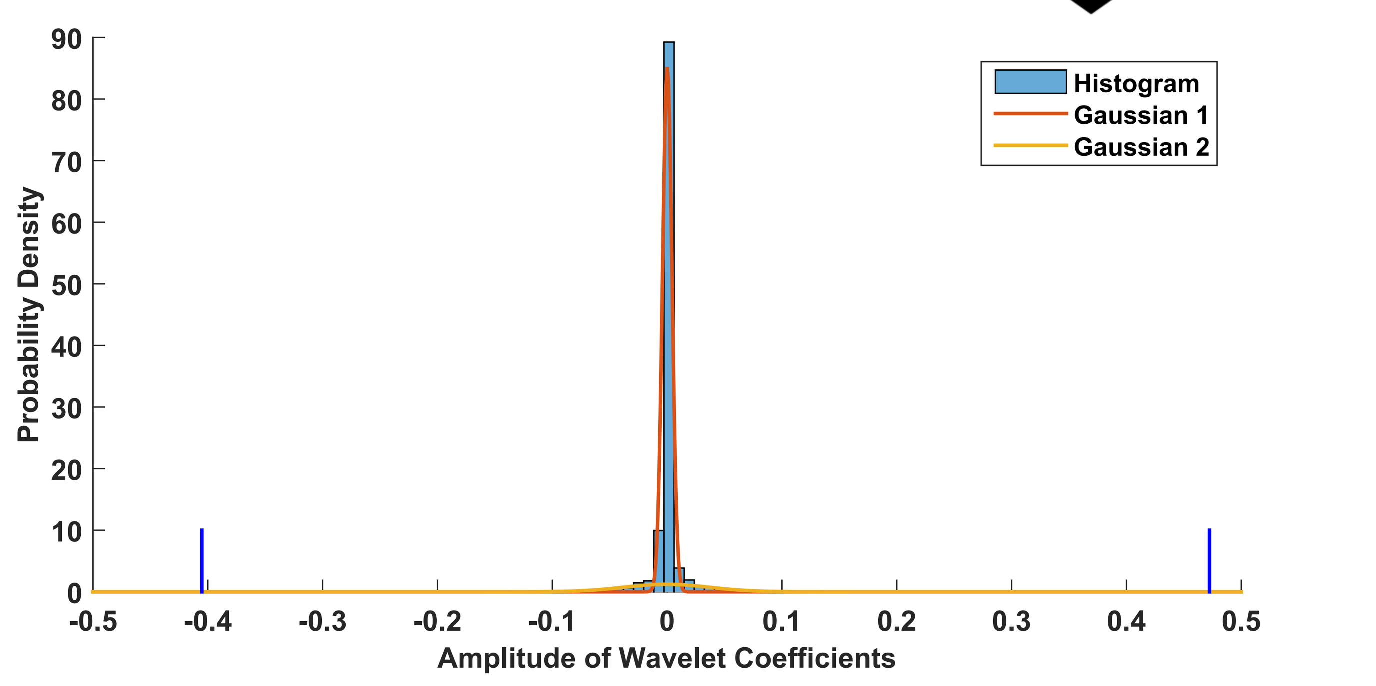

Figure 5. A typical histogram of the wavelet coefficients of an SC signal with a fitted model of two mixed Gaussians superimposed. The two blue vertical lines represent the minimum and maximum values of the histogram.

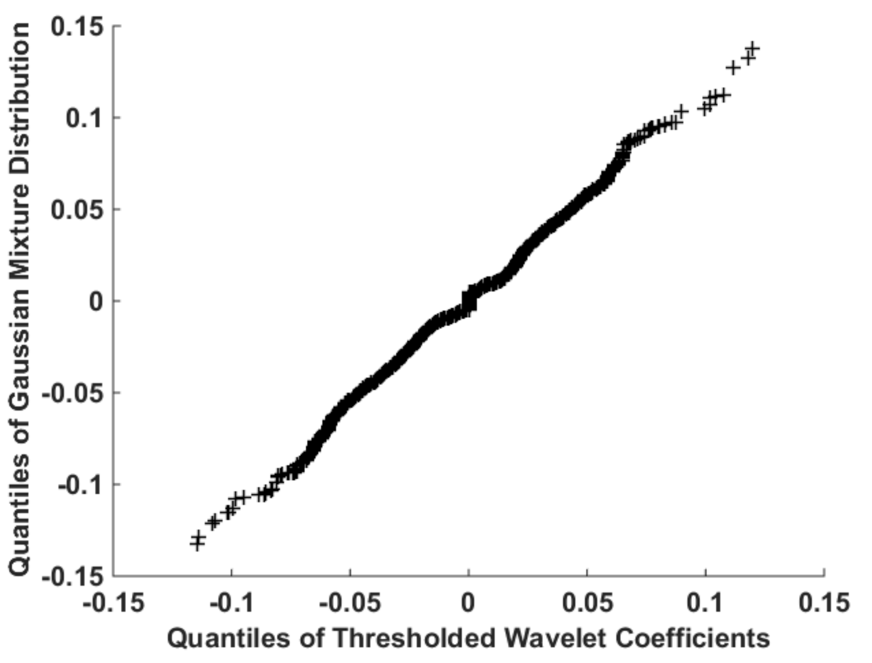

Figure 6. Q-Q plot of sample wavelet coefficients after thresholding versus a fitted Gaussian mixture distribution.

Results

- EDA data containing motion artifacts was obtained from a previous study [6], in which 32 subjects completed physical, cognitive and emotional tasks while wearing Q sensors on both wrists.
- During each trial, the Q sensors recorded SC, actigraphs (acceleration) and body temperature at a sampling frequency of 8 Hz for approximately 80 minutes.
- Two expert EDA researchers reviewed in total 61 records of data to manually label portions of the SC signals as containing motion artifacts.
- To quantitatively evaluate and compare the performance of all the methods, we used artifact power attenuation (APA) and normalized mean-squared error (NMSE) [14] as criteria:

$$APA_m = 10\log_{10}\frac{\sum_{n\in A_m} Var[y(n)]}{\sum_{n\in A_m} Var[\tilde{y}(n)]} \qquad NMSE = 10\log_{10}\frac{\sum_{n\notin A_m}[y(n)-\tilde{y}(n)]^2}{\sum_{n\notin A_m}[y(n)-\bar{y}(n)]^2}$$

Methods	Wavelet Thresholding	Hamming Filtering	Hanning Filtering	Exponential Smoothing
APA	6.3233	0.0233	1.2539	0.2559
NMSE	-54.4229	-54.4175	-48.1641	-57.5739

Table I. Median of NMSE and APA (in dB) for the evaluated methods.

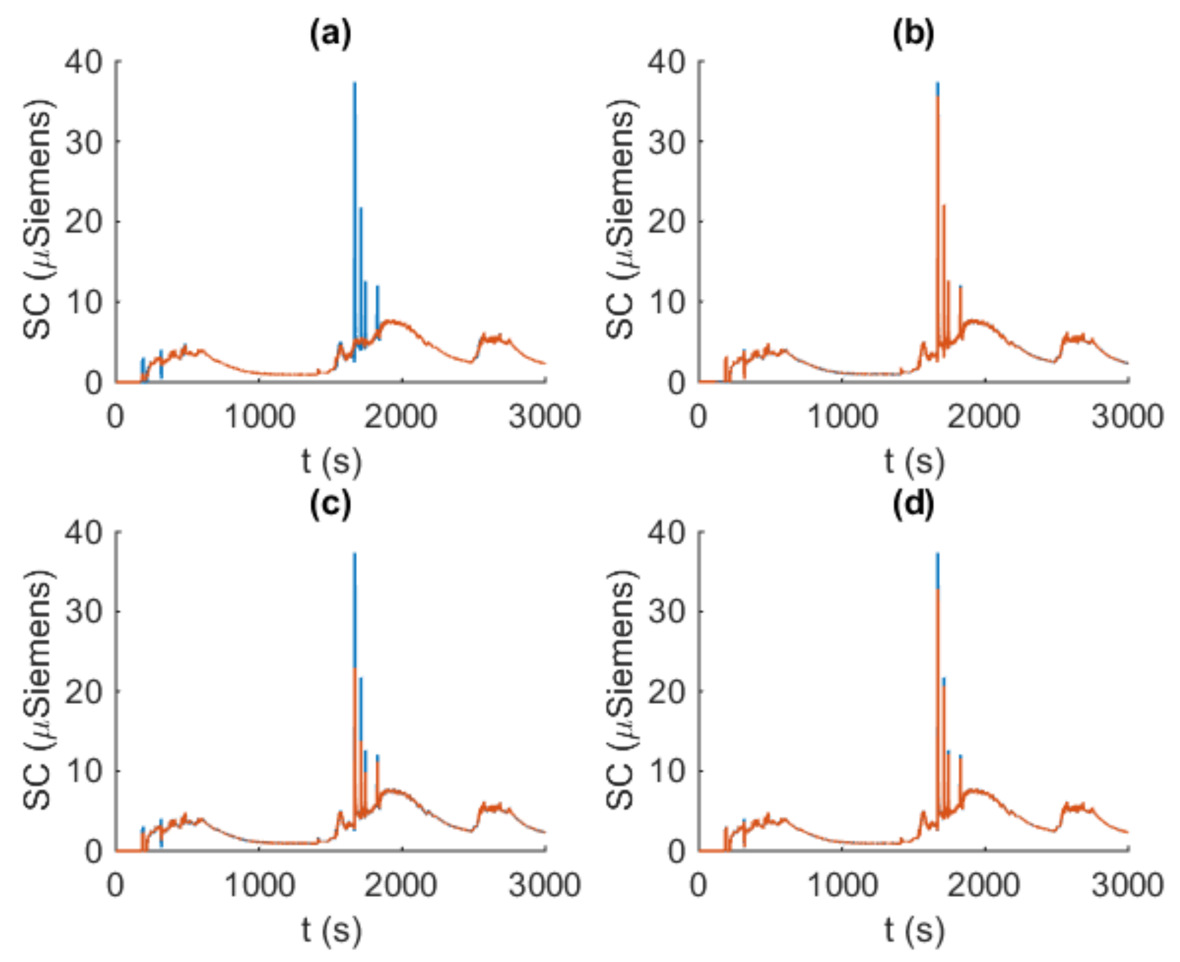

Figure 7. Original EDA (blue lines) and denoised signals (red lines) processed by (a) wavelet thresholding (Haar wavelet [18], artifact proportion δ = 0.01, time window length L = 400 seconds), (b) 1024-point low-pass Hamming filtering (cutoff frequency = 3 Hz) [15, 16], (c) Hanning filtering with a 1 second window [12] and (d) exponential smoothing (a = 0:8) [11].

[1] A. Antoniadis et al. Wavelet estimators in nonparametric regression: a comparative simulation study. J. of Stat. Software, 6(6):1–83, 2001.
[2] M. Benedek and C. Kaernbach. A continuous measure of phasic electrodermal activity. J. of neurosci. methods, 190(1):80–91, 2010.
[3] W. Boucsein. Electrodermal activity. Springer Science & Business Media, 2012.
[4] H. A. Chipman et al. Adaptive Bayesian Wavelet Shrinkage. J. of the American Statistical Association, 92 (440):1413–1421, 1997.
[5] R. Edelberg. Electrical properties of the skin. Methods in psychophysiology, pages 1–53, 1967.
[6] S. Fedor and R. Picard. Ambulatory EDA: Comparison of bilateral forearm and calf locations. In Society for Psychophysiological Research (SPR), Atlanta, 2014.
[7] D. C. Fowles et al. Publication recommendations for electrodermal measurements. Psychophysiology, 18 (3):232–239, 1981.
[8] J. Healey and R. Picard. Detecting stress during real-world driving tasks using physiological sensors. IEEE Trans. Intell. Transp. Syst., 6(2):156–166, June 2005.
[9] E. Hedman. The Frustration of Learning Monopoly : The Emotional Tension of Entering a New Game Encounter. In The Ethnographic Praxis in Industry Conference, Boulder, pages 18–21, 2011.
[10] E. Hedman et al. Measuring autonomic arousal during therapy. In Proceedings of 8th International Design and Emotion Conference, London, 2012.
[11] J. Hernandez et al. Call center stress recognition with person-specific models. Proceedings of the Affective Computing and Intelligent Interaction, Memphis, 2011.
[12] J. Hernandez et al. Using electrodermal activity to recognize ease of engagement in children during social interactions. In Int. Conf. on Ubiquitous Computing, Seattle, 2014.
[13] G. McLachlan and D. Peel. Finite mixture models. John Wiley & Sons, 2004.
[14] B. Molavi and G. A. Dumont. Wavelet-based motion artifact removal for functional near-infrared spectroscopy. Physiological Measurement, 33(2):259–270, 2012.
[15] M. Poh et al. A Wearable Sensor for Unobtrusive, Long-Term Assessment of Electrodermal Activity. IEEE Trans. Biomed. Eng., 57(5):1243–1252, 2010.
[16] M. Poh et al. Continuous monitoring of electrodermal activity during epileptic seizures using a wearable sensor. In 2010 Annual Int. Conf. of the IEEE Engineering in Medicine and Biology Society (EMBC), pages 4415–4418, 2010.
[17] A. Sano et al. Quantitative analysis of wrist electrodermal activity during sleep. Int. J. of Psychophysiology, 94(3):382–389, 2014.
[18] Y. Xu et al. Wavelet transform domain filters: a spatially selective noise filtration technique. IEEE Trans. Image Process., 3(6):747–758, 1994.